Asian Journal of Chemistry; Vol. 33, No. 12 (2021), 3075-3081

ASIAN JOURNAL OF CHEMISTRY

https://doi.org/10.14233/ajchem.2021.23439

Silver Doped Polyaniline-Graphene Based Barium Ferrite Composite as Humidity Sensor and Photocatalyst

K. VINAY[1], Y.T. RAVIKIRAN[2], M. REVANASIDDAPPA[3], A. NAVEEN KUMAR[4], K. VEENA[5], C.R. RAVIKUMAR[4,*] and H.C. ANANDA MURTHY[6,*]

[1]Department of Chemistry, Channabasaveswara Institute of Technology, Gubbi-572216, India
[2]Department of PG Studies & Research in Physics, Government Science College, Chitradurga-577501, India
[3]Department of Chemistry, PES University South Campus, Hosur Road, Bangalore-560100, India
[4]Research Centre, Department of Basic Science, East West Institute of Technology, (Affiliated to Visvesvaraya Technological University), Bangalore-560091, India
[5]Department of Chemistry, Maharani's Science College for Women, Bangalore-560001, India
[6]Department of Applied Chemistry, School of Applied Natural Science, Adama Science and Technology University, P.O. Box 1888, Adama, Ethiopia

*Corresponding authors: E-mail: ravicr128@gmail.com; anandkps350@gmail.com

Received: 27 July 2021; *Accepted*: 27 September 2021; *Published online*: 6 December 2021; AJC-20601

In this work, the response of humidity sensing and dielectric properties of PANI/Ag/graphene/$BaFe_{12}O_{19}$ (PAGB) composite prepared by chemical interfacial oxidative polymerization method using the ammonium peroxydisulfate as an oxidant is presented. The synthesized PAGB composite was characterized by using FT-IR, XRD, SEM and EDAX techniques. The measured dielectric constant and dielectric tangent loss values were found to decrease with increase in logarithmic frequency. The electrical resistance of the composite was also found to decrease from 2500 MΩ to 7 MΩ, on exposure to a wide range of relative humidity (RH) varying between 10% and 97% RH. This observed decrease is due to capillary condensation of water molecules which cause the changes in electrical conductivity of composite. The synthesized PAGB-50% composite displayed a high sensitivity at low humidity ranging from 20% to 60% RH. The composite has been proved to be a better candidate in the design of humidity sensors. In addition, PAGB composite exhibited efficiency towards the degradation of organic anionic dye, acid orange-8, with high potential of reusability.

Keywords: Composites, Barium ferrite, Polyaniline, Graphene, Humidity sensor, Acid orange 8 dye.

INTRODUCTION

The chemical sensors of humidity are incredibly significant to many sectors such as, industries, agriculture, storage of food, *etc*. They get better human comfort and well-being. A lot of sensors, based on ceramics [1], polymers [2] and composites [3] have been studied through the objective of good performance. The polymers based humidity sensors are the most preferred sensorscompared to other sensors due to their low cost, high-quality presentation, ease of manufacture and elevated sensitivity [4]. In addition, conducting polymers based nanomaterials were also applied to arrive at electrode materials due to the ease in the structural modifications. The conducting polymers were also proved to exhibit good mechanical strength. As a consequence of better properties of conducting polymers, commercial sensors fabricated from conducting polymers gained significant attention. Polyaniline is one such simple conducting polymer, which can be prepared without any sophisticated lab requirements. The large number of research papers that describe PANI synthesis have been found in the literature [5-8]. PANI based composites decorated with inorganic nanoparticles are of great interest since potential interactions between inorganic nanoparticles and polymer matrices can lead to novel polymer composites with super-functional properties such as thermal and chemical stability, tunable conductivity and low specific mass [9]. Recently, barium hexaferrite ($BaFe_{12}O_{19}$) has been of a great interest because of its high magnetic anisotropy and high packing density, which

finds applications in diverse areas such as permanent magnets, magnetic card strips, loud speakers, magnetic tapes, microwave devices and EMI shielding [10]. These materials have proven record of exhibiting superior resistance to various environmental stresses, such as temperature, humidity and corrosion. It is readily evident that metals combined with graphene, doped with single transition metal atom catalysts and prepared as electrocatalytic sensors can be employed to enhance some unique properties different from properties of bulk graphene. Thus, the synthesis and design of metal silver doped PANI-graphene-$BaFe_{12}O_{19}$ composite [11] is of great importance for the development of new material for the scientific community in current years due to their potentiality towards the future generation electronic devices, opto-electronics, sensors, electrical-magnetic shields, microwave absorbing materials, batteries, corrosion protections and liquid crystal devices.

EXPERIMENTAL

The chemicals used were of analytic reagent grade. Aniline (99.5%) monomer was double distilled prior to use. Ammonium peroxydisulphate ($(NH_4)_2S_2O_8$; 98%), chloroform, barium ferrite (99.5%) and nitric acid (99%) of S.D. fine chemicals were used as obtained. Graphene nanopowder was procured from Adman nano Technologies. Milli-Q water, an ultra-pure water was used for dissolution purpose.

Preparation of silver doped PANI-graphene-$BaFe_{12}O_{19}$ composite: Aniline (0.1 M) was dissolved in nitric acid solution (1 M) in a beaker containing 10 mL chloroform. Then $(NH_4)_2S_2O_8$ (0.1 M) solution and 0.1 M silver nitrate (99%) solution were separately mixed along the sides of the beaker, slowly beginning oxidation at room temperature for around 4-6 h, resulted in the slow formation of a dark green coating at the immiscible interface and then eventually spreading into the aqueous phase. The aqueous phase was then extracted and washed with ethanol after 24 h resulted in the formation of a polyaniline matrix doped with glossy silver particles. $BaFe_{12}O_{19}$ powder was spread with constant stirring in a polymer solution to hold the particles of $BaFe_{12}O_{19}$ suspended in the solution. The reaction mixture was allowed to settle at 5 ºC. The acquired precipitation was vacuum-filtered, then washed with milli-Q water followed by acetone. The resulting product was dried to gain constant weight in an oven at 70 ºC.

Following this process, various composites of PANI/Ag/$BaFe_{12}O_{19}$ (PAB) were prepared with $BaFe_{12}O_{19}$ in PANI/Ag matrix by 10%, 20%, 30%, 40% and 50% by weight. In the required solvent method with acetone, different compositions of PAGB 10%, 20%, 30%, 40% and 50% composites were combined mechanically with graphene nanopowder. The obtained final product was fine grained to get powdered composites and used for further characterization studies.

Electrical measurements: The electrical measurements for the synthesized PAGB samples were carried out using the HIOKI 3532-50 LCR Hi-tester at room temperature in the frequency range $5 \times 10^1 - 5 \times 10^6$ Hz. The obtained powder samples were pressed to form pellets with a diameter of 10mm and a thickness of 1.5 mm by applying a hydraulic pressing having a pressure of 95 MPa. To achieve stronger electrical contact, the pellets were subjected to surface coating using the silver paste.

Humidity sensing measurements: All the measurements of the humidity response of synthesized PAGB composites were carried out at room temperature using the Mextech-DT-615 instrument. By dispersing the PAGB composites in *m*-cresol, thin free-standing films of bulk PANI and its composites were prepared and then smeared on petri dish to obtain a thin film of 1-2 μm thickness using a spin-coating unit (Model: Delta Spin I; Make: Delta Scientific Pvt. Ltd, India). Then, in a glass chamber retaining the desired relative humid environment, the film on interdigitated silver electrode was impregnated for good electrical contact.

RESULTS AND DISCUSSION

FTIR studies: The major peaks of PANI observed in the FT-IR spectrum of PAGB-50% composite were in compliance with the values reported earlier [12]. In the composite, the corresponding band assignments are shown in Table-1. The C-H stretching of sp^2 hybridized carbon is responsible for the characteristic vibrations at 3417 and 1570 cm^{-1} due to absorbed moisture and skeletal vibrations of unoxidized graphene nanosheets [13] and extra band at 2921 cm^{-1}. In Fig. 1a, the absorption bands observed at 578 and 428 cm^{-1} correspond to typical Fe–O bond stretching in the $BaFe_{12}O_{19}$ structure [14] and refers tetrahedral and octahedral sites vibrations of $BaFe_{12}O_{19}$, respectively. The observation of characteristic stretching frequencies of PANI and $BaFe_{12}O_{19}$ exhibit a slight red shift, substantiates well encapsulation of PANI particles in $BaFe_{12}O_{19}$ [15] through careful observation of the composite FT-IR spectra.

TABLE-1
IR BANDS AND ITS ASSIGNMENTS OF
PANI IN THE PAGB-50% COMPOSITE

IR bands (cm^{-1})	Band assignments
3227	N–H stretching of aniline
1490	C=C stretching of quinoid moiety
1445	C=C stretching of benzenoid unit
1300	C-N stretching of benzenoid ring
1240	Protonated form of IPANI
1105	N=Q=N vibrational mode
822	C-H out-plane deformation of benzene ring

XRD studies: The XRD diffraction peaks of $BaFe_{12}O_{19}$ (Fig. 2) centered at $2\theta = 30.3°$ (d = 2.94 Å), 32.1° (d = 2.77 Å), 34.1° (d = 2.62 Å), 37.1° (d = 2.42 Å), 40.3° (d = 2.23 Å), 42.4° (d = 1.66 Å), 55.0° (1.66 Å), 56.5° (d = 1.62 Å) and 63.0° (d = 1.47 Å) referred to diffractionof planes (110), (107), (114), (203), (205), (206), (217), (20 11) and (220), respectively can be indexed to the hexagonal lattice structure of barium ferrite (JCPDS card No.43-2 (space group $P6_3/mmc$ no.194). All the characteristic peaks found in the XRD pattern of $BaFe_{12}O_{19}$ fit well and are in good agreement with the values reported in the literature [15]. The XRD spectrum of PAGB composite (Fig. 2) displays well-retained peaks of $BaFe_{12}O_{19}$ characteristics, but a decrease in the intensity of the prominent peaks of $BaFe_{12}O_{19}$ and some low intensity peaks were also suppressed by the coated PANI layer. Additionally, compared with the diffraction

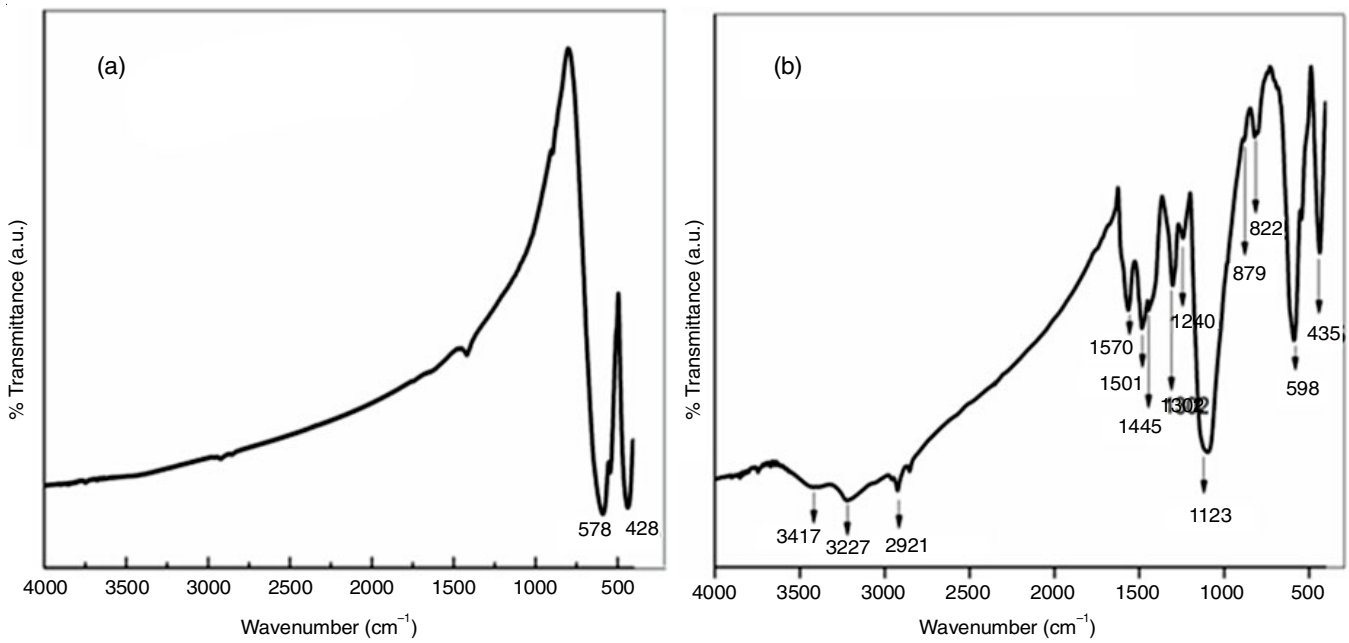

Fig. 1. FT-IR spectra of (a) $BaFe_{12}O_{19}$, (b) PAGB-50% composite

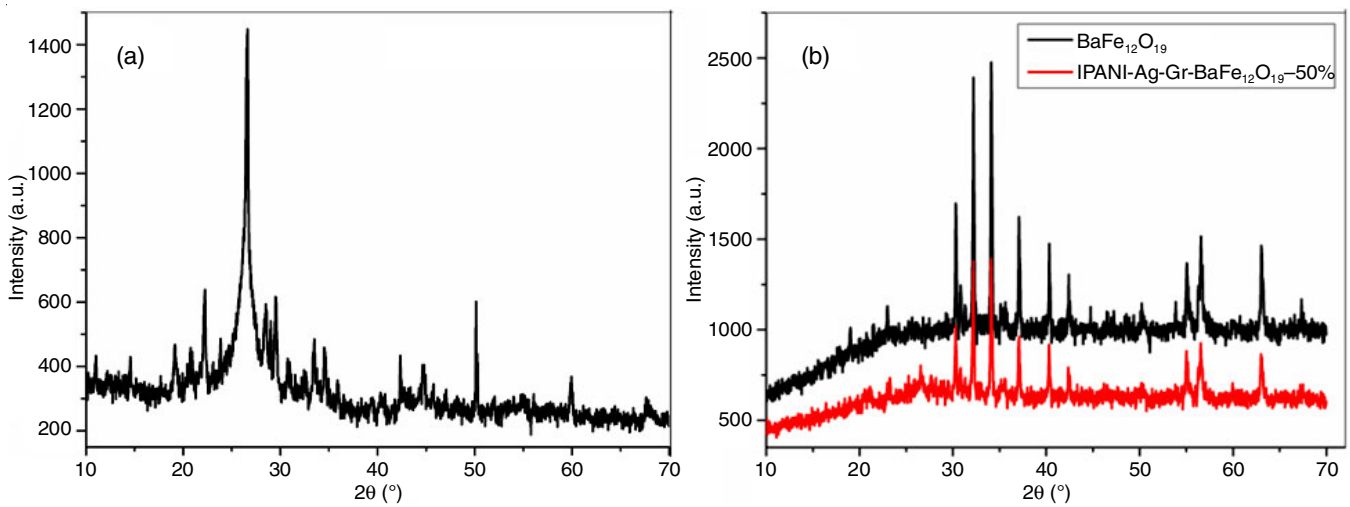

Fig. 2. XRD spectra of (a) graphene nanoparticle (b) $BaFe_{12}O_{19}$ and PAGB-50% composite

spectrum $BaFe_{12}O_{19}$, the strength of most of the characteristic peaks of the composite was diminished, which shows that the synthesized composite crystallinity has been fainted [16].

Graphene exhibited a characteristic large and extreme peak at the diffraction angle 2θ = 26.50º corresponding to the diffraction plane (003) and can be indexed to the rhombohedral phase of graphene, which is in compliance with JCPDS pattern No. 26-1079 (space group *R*3 no. 146). Due to the (003) reflection plane, the characteristic wide band peak of graphene at 2θ = 26.50º was clearly observed in the composite XRD pattern, which confirms the prescence of graphene in composite [17].

The lattice volume V, of rhombohedral phase of graphene nanoparticle is 52.46 Å (a = 2.456 Å; c = 10.044 Å) calculated using eqn. 1:

$$V = \frac{\sqrt{3}}{2} a^2 c \quad (1)$$

where a and c are lattice constants. The Inter-gallery distance between the graphene sheets was calculated by using Bragg's equation (eqn. 2):

$$\lambda = 2d \sin \theta \quad (2)$$

where d is the spacing between sheets; λ is the wavelength of X-ray; and θ is the angle of diffraction.

The inter-gallery distance between the graphene sheets was deduced to be 0.3359 nm. Using the Debye-Scherer's formula [18], the mean crystallite particle size of the polymer samples under investigation was measured using eqn. 3:

$$D = \frac{k\lambda}{\beta \cos \theta} \quad (3)$$

where D is the average particle crystallite size, λ = 0.154 nm (Cu*K*α radiation source X-ray wavelength), K = 0.89 is the form factor that depends on the form of the reflecting planes crystal and Miller Index, θ is half the diffraction angle and β

is maximum width at half the diffraction peaks in radians. Table-2 shows that the introduction of $BaFe_{12}O_{19}$ particles into the PANI matrix decreases the composite material's crystallite size. The mixing polymer with ferrite content therefore decreases the growth of the grain, which in turn reduces the particle's grain size.

TABLE-2
AVERAGE CRYSTALLITE PARTICLE SIZE OF THE SAMPLE MATERIAL BY USING DEBYE-SCHERER RELATION

Sample	hkl	θ (rad)	β (rad)	D (nm)
$BaFe_{12}O_{19}$	114	0.2983	0.0018	73.7
PAGB-50%	114	0.2983	0.0023	59.6

SEM studies: The SEM image (Fig. 3) displays agglomerated particles of $BaFe_{12}O_{19}$, most of which are elongated with a platelet like hexagonal shapes in a diameter range of 1-5 μm. $BaFe_{12}O_{19}$ exhibited a hexagonal crystal structure characterized by two lattice parameters, hexagonal plane width a = 0.5892 nm and crystal height c = 2.3183 nm. This correlates with the XRD findings, agglomeration of $BaFe_{12}O_{19}$particles can appear due to the interaction between magnetic ferrite particles with high surface energy [19].

The SEM micrographs of PAGB 50% composite show irregularly formed particles with few PANI particle on the surface $BaFe_{12}O_{19}$ hexagonal flakes, due to *in situ* polymerization agglomeration. The micrographs clearly show that the hexagonal platelet particles coated with small grains of PANI were successfully decorated with the graphene template. It is also worth noting that interactions between grapheme sheets and hexagonal $BaFe_{12}O_{19}$ can occur with van der Waals forces.

EDX analysis: The stoichiometric ratios of the main metallic components and components of the synthesized polymer composite are shown in Tables 3 and 4. The quantity of N was found to be greater in PANI bulk and decreased further when silver, $BaFe_{12}O_{19}$ and graphene nanoparticles were integrated [20]. The corresponding EDX spectra showed the typical peaks

TABLE-3
WEIGHT (%) OF Ba, Fe, Ag AND ELEMENTS (C, N AND O) OBTAINED FROM EDX ANALYSIS

Sample	EDAX (weight %)					
	C	N	O	Ba	Fe	Ag
IPANI	48	13	39	0	0	0
IPANI-Ag	65	8.5	25	25	0	1.5
$BaFe_{12}O_{19}$	0	0	19	19	34	0
PAGB 50%	58	5	23.9	2	10	1.1

TABLE-4
ATOM (%) OF Ba, Fe, Ag AND ELEMENTS (C, N AND O) OBTAINED FROM EDX ANALYSIS

Sample	EDX (atomic %)					
	C	N	O	Ba	Fe	Ag
IPANI	54	14	32	0	0	0
IPANI-Ag	74	4	21.5	0	0	0.5
$BaFe_{12}O_{19}$	0	0	57	38	0	0
PAGB 50%	68	6.4	22	1.3	1.7	0.4

of element Ba, Fe and O. Fig. 4a shows a representative EDX spectrum of bulk $BaFe_{12}O_{19}$. No more impurity peaks were found. To determine its chemical composition, the EDX spectrum of PAGB50% composite was recorded (Fig. 4b) and it showed that the composite was composed primarily of elements Ag, Ba, C, O, N and Fe. There were characteristic peaks of elemental C, Ba, Fe, O, N and Ag in the corresponding EDX spectra. All the peaks associated with the elements of barium ferrite such as iron, barium and oxygen were observed. In composite, Ba, Fe and O ratios confirmed the formation of the barium hexaferrite structure.The introduction of $BaFe_{12}O_{19}$ into the silver doped PANI matrix decreases the content of Ba and Fe accordingly, revealed that there is an interaction between particles of $BaFe_{12}O_{19}$ and PANI and confirming the composite formation.The EDX spectrum shows clearly that due to the inclusion of graphene nanoparticle in the PANI barium ferrite matrix, the atomic % of C was found to increase by 27%.

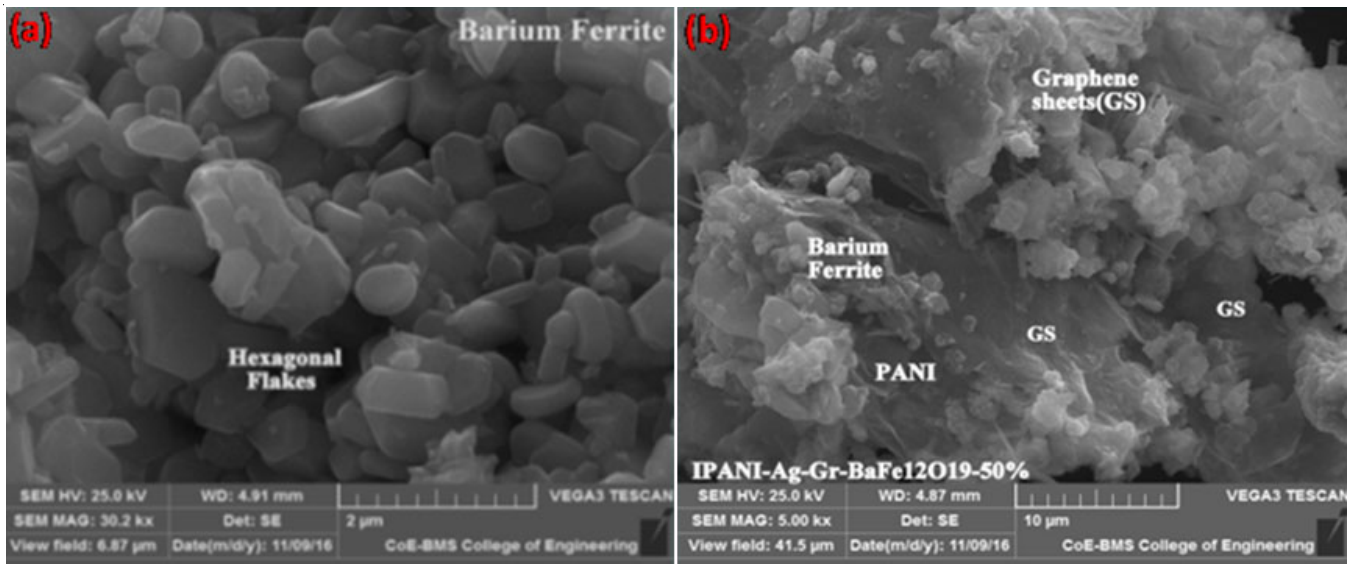

Fig. 3. SEM micrographs of (a) $BaFe_{12}O_{19}$ (b) PAGB-50% composite

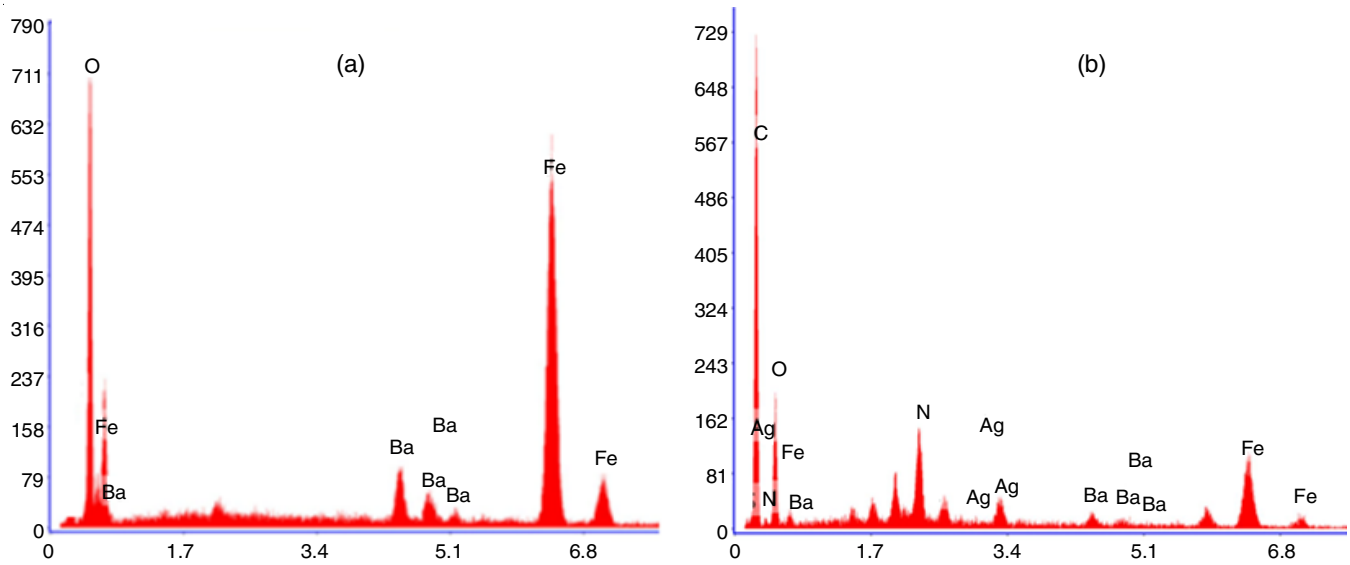

Fig. 4. EDX spectra of (a) $BaFe_{12}O_{19}$ and (b) PAGB-50% composite

Photocatalytic activity: The photocatalytic analyses were achieved for degradation of acid orange 8 (AO8) dye, a 20 ppm of 250 mL aqueous solution of AO8 dye and 60 mg of photocatalysts in the reactor. The UV light irradiation into the reaction mixture has been achieved from a height of 23 cm in the open-air condition [21,22]. Likewise, it was supervised by UV-vis absorption spectroscopy at room temperature in the range of 200-800 nm using Shimadzu UV-Vis spectrophotometer model 2600.

The photocatalytic activity of PAGB composite was studied by the decolorization of acid orange 8 dye, an anionic dye with maximum absorption at 483 nm as shown in Fig. 5a. Initially, the photocatalytic activity were carried out in the dark condition to see the photocatalytic activity of the dye using the synthesized catalysts. The dye did not undergo any degradation and hence, no change was observed.

At last, the photocatalytic experiments were conducted under UV light irradiation at a concentration of 20 ppm by using 60 mg of silver doped PANI-graphene-$BaFe_{12}O_{19}$ as a catalyst for decolourization of dye up to 2 h. The degree of adsorption (Q) was estimated by using the eqn. 4:

$$Q = \frac{(C_o - C)V}{W} \quad (4)$$

During the first 15 min, the decolourization of dye was recorded to be 12% and in the subsequent measurements at 30, 45, 60, 75, 90, 105 and 120 min, AO8 dye exhibited a further decolou-rization resulting in 19.7, 29.5, 36.15, 46.15, 50, 56.15 and 60%, respectively (Fig. 5b). The percentage of degradation of dye was calculated using eqn. 5:

$$D\ (\%) = \frac{C_o - C}{C_o \times 100} \quad (5)$$

where % D is the photo-decolorization efficiency, C_o and C are the initial concentration of the dye solution and the residual concentration of the dye in solution after decolorization in equilibrium, respectively [23].

Fig. 5c reveals the plot of (C/C_o) *versus* time which indicates that the degradation increased with time and was maximum at 120 min. Further, C/C_o values were also calculated by eqn. 6:

$$\frac{\log C}{C_o} = -Kt \quad (6)$$

where C_o and C are the concentrations of dye at time t = 0 min and at the time of testing, respectively and k is the first order rate constant.

The deduced values revealed a linear relationship of log C/C_o and k confirmed the first order kinetics. The slope k was

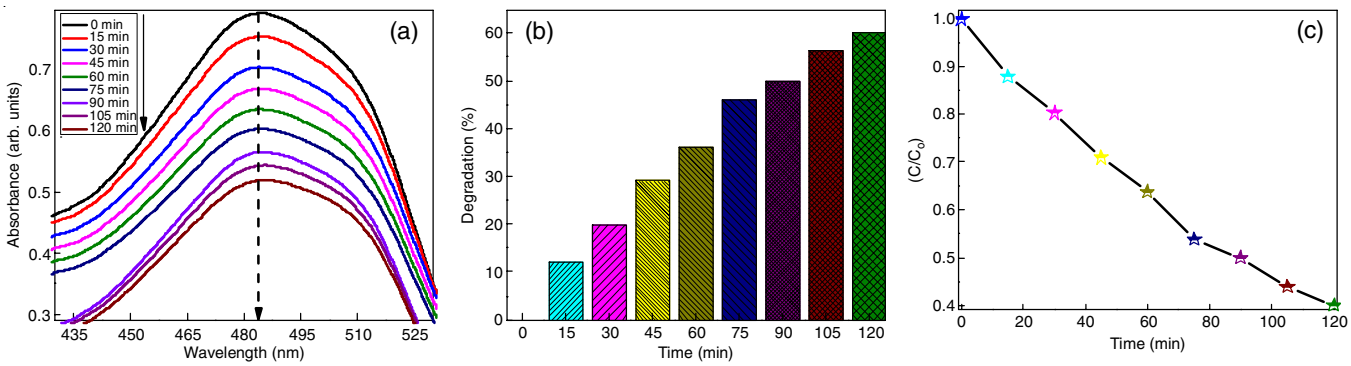

Fig. 5(a). Absorption spectra of acid orange 8 (b) plot of% decolorization of acid orange 8 under UV light (c) plot of (C/C_o) *versus* time

found to be 0.007419 min^{-1} for acid orange 8 dye (Table-5). The results indicated that the silver doped PANI-graphene-$BaFe_{12}O_{19}$ as a photocatalyst can be a potential candidate for the degradation of organic anionic dye with high potential of reusability and are also useful for the removal of secondary pollutants.

Humidity sensing behaviour: Due to the capillary condensation of water molecules and the polarization mechanism, the resistance of the samples under investigation showed a decreasing trend with the rise in the humid environment (Fig. 6). The PAGB and PAGB50% composite showed strong response up to 97% maximum humidity, but stability was lost over 76% RH and then begins the degradation [24]. Fig. 6 inset, depicts the resistance variation as a function of relative humidity for bulk PANI. With a rise in humidity, PANI shows almost linear downtrend electrical resistance. The polymer chains will appear to curl up in a convenient compact coil shape under dry circumstances. On the contrary, the PANI composite absorbs water molecules at high humidity, resulting in the uncurling of the shape of the compact coil into straight chains aligned with each other [25,26]. The PAGB50% composite displays non-linear rapid response in the RH range from 20% to 70%. Moreover, when the composite was exposed to a large range of relative humidity ranging from 10% to 97%, a decrease in electrical resistance from 2500-7 MΩ was observed, indicating strong sensitivity, which indicates the composite's liability to humidity.

Conclusion

In this study, the PANI/Ag/graphene/$BaFe_{12}O_{19}$ (PAGB) composite was successfully synthesized by *in situ* chemical oxidative interfacial polymerization. The FTIR spectra of the composite confirmed the effective bonding interactions among various groups. The XRD results revealed that the incorporation of $BaFe_{12}O_{19}$ in to the PANI matrix decreases the crystallite size of the composite. The resistive humidity sensitivity of the PAGB-50% composite film was investigated and downfall in the electrical resistance was observed from 2500-7 MΩ as relative humidity increases from 10% to 97%. A stable performance of the PAGB composite in sensing the humidity was observed with no deterioration corroborating that the composite acts as a better candidate in the design of humidity sensors.In addition, PAGB composite acts as an efficient photocatalyst towards the degradation of organic anionic dye with high potential of reusability.

TABLE-5
RATE CONSTANTS AND KINETIC STUDIES OF SILVER DOPED IPANI-GRAPHENE-$BaFe_{12}O_{19}$ FOR ACID ORANGE-8 (AO8) DECOLORIZATION UNDER UV LIGHT

(A) 20 ppm Acid orange-8 (AO8) + 60 mg (silver doped IPANI-graphene-$BaFe_{12}O_{19}$) + UV light

T	c	c/c_o	log c/c_o	-log c/c_o	%D
0	20.00	1.0000	0	0	0
15	17.60	0.8800	-0.05552	0.055517	12.00
30	16.06	0.8030	-0.09528	0.095284	19.70
45	14.19	0.7095	-0.14905	0.149048	29.05
60	12.77	0.6385	-0.19484	0.194839	36.15
75	10.77	0.5385	-0.26881	0.268814	46.15
90	10.00	0.5000	-0.30103	0.301030	50.00
105	8.77	0.4385	-0.35803	0.358030	56.15
120	8.00	0.4000	-0.39794	0.397940	60.00

Rate = 0.007419 min^{-1}

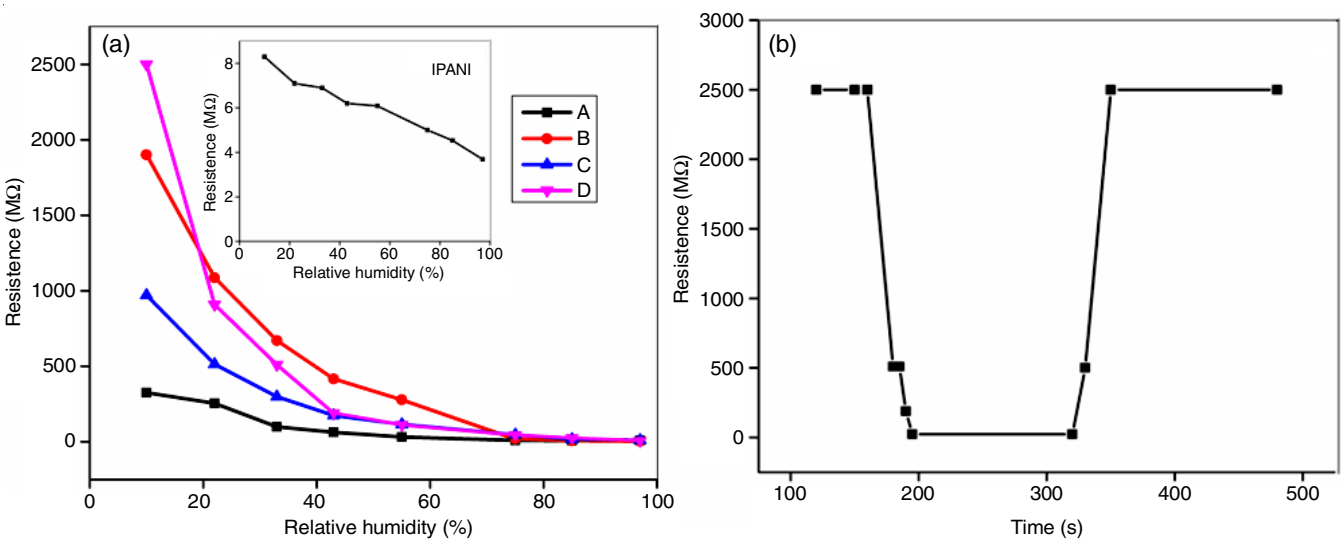

Fig. 6. (a) Variation of electrical resistance as a function of % relative humidity for (A) $BaFe_{12}O_{19}$, (B) IPANI/Ag, (C) IPANI/Ag/graphene (PAG) (D) PAGB-50% composite and for the bulk IPAN (b) Response and recovery characteristic curve of PANI/Ag/graphene/$BaFe_{12}O_{19}$(PAGB)-50% composite at 25 °C

CONFLICT OF INTEREST

The authors declare that there is no conflict of interests regarding the publication of this article.

REFERENCES

1. W. Zhang, L. Chen, Z. Yang and J. Peng, *Sens. Actuators B Chem.*, **155**, 226 (2011); https://doi.org/10.1016/j.snb.2010.11.052
2. T. Wang, N. Zhang, W. Bai and Y. Bao, *Polym. Chem.*, **11**, 3095 (2020); https://doi.org/10.1039/D0PY00336K
3. R.P. Tandon, M.R. Tripathy, A.K. Arora and S. Hotchandani, *Sens. Actuators B Chem.*, **114**, 768 (2006); https://doi.org/10.1016j.snb.2005.07.022
4. T. Sakai, M. Hamakawa and S. Kubo, *J. Dairy Sci.*, **79**, 372 (1996); https://doi.org/10.3168/jds.S0022-0302(96)76374-9
5. S. Ameen, M.S. Akhtar and M. Husain, *Sci. Adv. Mater.*, **2**, 441 (2010); https://doi.org/10.1166/sam.2010.1126
6. M. Beygisangchin, S.A. Rashid, S. Shafie, A.R. Sadrolhosseini and H.N. Lim, *Polymers*, **13**, 2003 (2021); https://doi.org/10.3390/polym13122003
7. J. Bhadra, A. Alkareem and N. Al-Thani, *J. Polym. Res.*, **27**, 122 (2020); https://doi.org/10.1007/s10965-020-02052-1
8. V. Babel and B.L. Hiran, *Polym. Compos.*, **42**, 3142 (2021); https://doi.org/10.1002/pc.26048
9. N. Parvatikar, S. Jain, C.M. Kanamadi, B.K. Chougule, S.V. Bhoraskar and M.A. Prasad, *J. Appl. Polym. Sci.*, **103**, 653 (2007); https://doi.org/10.1002/app.23869
10. Y. Yang, M.C. Gupta, K.L. Dudley and R.W. Lawrence, *J. Nanosci. Nanotechnol.*, **5**, 927 (2005); https://doi.org/10.1166/jnn.2005.115
11. S.M. Hosseini, N. Rafiei, A. Salabat and A. Ahmadi, *Arab. J. Chem.*, **13**, 2470 (2020); https://doi.org/10.1016/j.arabjc.2018.06.001
12. S. Shahabuddin, N.M. Sarih, M.A. Kamboh, H.R. Nodeh and S. Mohamad, *Polymers*, **8**, 305 (2016); https://doi.org/10.3390/polym8090305
13. M. Mallesha, R. Manjunatha, G.S. Suresh, J.S. Melo, S.F. D'souza and T.V. Venkatesha, *J. Solid State Electrochem.*, **16**, 2675 (2012); https://doi.org/10.1007/s10008-012-1674-y
14. M.H. Zahari, B.H. Guan, E.M. Cheng, M.F. Che Mansor and H.A. Rahim, *Progr. Electromag. Res.*, **52**, 111 (2016); https://doi.org/10.2528/PIERM16100402
15. D. Shekhawat, S. Verma and P. Sharma, *Trans. Indian Ceram. Soc.*, **76**, 247 (2017); https://doi.org/10.1080/0371750X.2017.1396925
16. D.S. Bai, R.P. Suvarna and B.M. Nagabhushana, *Mater. Today Proc.*, **5**, 20793 (2018); https://doi.org/10.1016/j.matpr.2018.06.464
17. B.M. Chufa and H.A. Murthy, *J. Mater. Environ. Sci.*, **11**, 844 (2020).
18. A. Rakita, N. Nikolic, M. Mildner, J. Matiasek and A. Elbe-Bürger, *Sci. Rep.*, **10**, 1 (2020); https://doi.org/10.1038/s41598-019-56847-4
19. M. Kumar and B.E.K. Swamy, *Mater. Sci. Eng. C*, **58**, 142 (2016); https://doi.org/10.1016/j.msec.2015.08.002
20. R.J. Ramalingam, H.A. Al-Lohedan and T. Radhika, *Dig. J. Nanomater. Biostruct.*, **11**, 731 (2016).
21. M.A. Kumar, C.R. Ravikumar, H.P. Nagaswarupa, B. Purshotam, B. Gonfa, H.A. Murthy, F.K. Sabir and S. Tadesse, *J. Environ. Chem. Eng.*, **7**, 103468 (2019); https://doi.org/10.1016/j.jece.2019.103468
22. K.M. Girish, S.C. Prashantha, H. Nagabhushana, C.R. Ravikumar, H.P. Nagaswarupa, R. Naik, H.B. Premakumar and B. Umesh, *J. Sci.: Adv. Mater. Devices*, **3**, 151 (2018); https://doi.org/10.1016/j.jsamd.2018.02.001
23. P. Zhang, C. Shao, M. Zhang, Z. Guo, J. Mu, Z. Zhang, X. Zhang, P. Liang and Y. Liu, *J. Hazard. Mater.*, **229-230**, 265 (2012); https://doi.org/10.1016/j.jhazmat.2012.05.102
24. S.C. Nagaraju, A.S. Roy, J.B. Kumar, K.R. Anilkumar and G. Ramagopal, *J. Eng.*, **2014**, 925020 (2014); https://doi.org/10.1155/2014/925020
25. K.C. Sajjan, A.S. Roy, A. Parveen and S. Khasim, *J. Mater. Sci. Mater. Electron.*, **25**, 1237 (2014); https://doi.org/10.1007/s10854-014-1715-7
26. G.R. Chaudhary, S. Bansal, P. Saharan, P. Bansal and S.K. Mehta, *BioNanoSci.*, **3**, 241 (2013); https://doi.org/10.1007/s12668-013-0094-5